THEORY OF A GAS LASER WITH NONLINEAR ABSORPTION

A. P. KAZANTSEV, S. G. RAUTIAN and G. I. SURDUTOVICH

Institute of Semiconductor Physics, Siberian Division, USSR Academy of Sciences

Submitted November 1, 1967

Zh. Eksp. Teor. Fiz. 54, 1409–1421 (May, 1968)

The theory of a gas laser with an absorbing cell within the resonator is discussed. The point of departure is the concept of a nonomonotonic dependence of the effective gain of such a system on the squared field amplitude E^2. The concept is used in the qualitative interpretation of the hysteresis phenomenon (lack of coincidence between the beginning and end of generation observed in frequency scanning or population variation in the active or passive components of the laser) discovered by Lisitsyn and Chebotaev[1,2]. A quantitative analysis is performed in the simplest approximation consisting in retaining the $\sim E^4$ terms in the effective gain expansion. The output power as a function of frequency and the number of active and absorbing particles is investigated.

LISITSYN and Chebotaev[1,2] recently experimented with a He-Ne laser (λ = 6328 Å) that contained a neon absorption cell along with the active medium within the resonator. When a single mode is generated and the cell absorption is sufficiently high the plot of emission power ϵ as a function of frequency Ω has a more or less pronounced maximum near the transition frequency; the maximum vanishes when the absorption is low (Fig. 1a). The plot of $\epsilon(\Omega)$ is asymmetric and the peak width depends on output power. When the absorption is increased further the plot of $\epsilon(\Omega)$ shows a hysteresis: the start and end of generation depend on the direction of frequency scanning. A similar pattern of generation power behavior is also observed when other parameters of the system are varied, such as the discharge current I in the active medium (Fig. 1b)[1)].

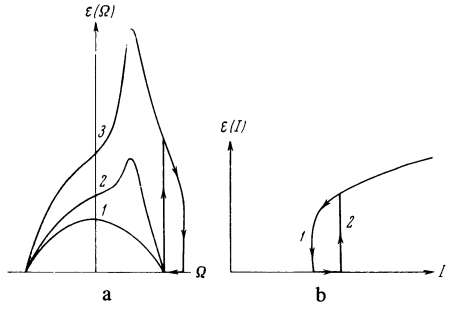

FIG. 1. a – Generation power ϵ as a function of frequency Ω. The frequency scanning direction is indicated by arrows in curve 3. Curves 1, 2, 3 appear with increasing absorption. Gain is increased here in a corresponding manner. b–Generation power ϵ as a function of the discharge current in the active laser component. Arrows indicate the direction of current variation.

1. INTRODUCTION

This paper presents the theory of the effects observed by Lisitsyn and Chebotaev. We essentially consider the theory of a gas laser, taking account of the saturation effect in the absorbing medium. The presence of hysteresis in the output power can be qualitatively explained in the following manner. In the stationary generation regime the electric field amplitude E can be found by equating gains and losses in the system:

$$\alpha_1(E^2) - \alpha_2(E^2) = f. \qquad (1.1)$$

Here α_1 and α_2 are the products of gain and absorption coefficients for the lengths l_1 and l_2 of the active and absorbing media of the laser respectively, and f are the resonator losses. Since the function $\alpha_1(E^2)$ decreases monotonically (curve 1, Fig. 2) the solution of (1.1) in the absence of absorption ($\alpha_2 = 0$) is unique if it exists at all. In addition to the solution E_1^2 there is also a stationary state, E = 0, of the system. This state, however, is unstable if the gain $\alpha_1(0)$ in zero field exceeds the losses f. Therefore in the absence of absorption the amplitude E is always uniquely determined by (1.1) if $\alpha_1(0) > f$, and is zero if $\alpha_1(0) < f$.

On the other hand, the presence of hysteresis in some frequency range (Fig. 1a) and in a definite interval of the discharge current values (Fig. 1b) points to the existence of two stable states of the system, one of which is the zero-amplitude state. The stability of the E = 0 state clearly requires that losses in the resonator exceed the difference between gain and absorption in the zero field. Consequently in the region of the hysteresis $\alpha_1(0) - \alpha_2(0) < f$. Furthermore, (1.1) must have a stable solution. Figure 2 (curve 4) shows the simplest form of $\alpha_1 - \alpha_2$, as a function of field amplitude, which satisfies these two conditions. In this situation the states E = 0 and $E = E_4$ are stable and the state with amplitude E_4' is unstable. Such a nonmonotonicity of the function $\alpha_1(E^2) - \alpha_2(E^2)$ will be shown to be capable of providing a qualitative explanation for all the basic experimental results of Lisitsyn and Chebotaev[1,2]. We note that a plot of this type is possible under their experimental conditions if the pressures and currents in the active and absorbing

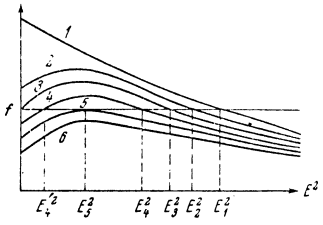

FIG. 2. Plot of effective gain $\alpha_1 - \alpha_2$ as a function of squared electric field amplitude E.

[1)]The peak in the $\epsilon(\Omega)$ plot was also recently observed by Lee and Skolnick [3].

components of the laser are suitably adjusted. As we know the collision width γ, lifetimes γ_m^{-1} and γ_n^{-1} of the atom at the levels m and n, and the saturation parameter $\sigma = 2d^2h^{-2}\gamma^{-1}(\gamma_m^{-1} + \gamma_n^{-1})$ depend on pressure (d is the matrix element of the dipole moment). If the gas pressure in the absorption cell is much lower than in the active medium there will be a large difference between their saturation parameters: $\sigma_1 \ll \sigma_2$. Therefore the field dependence of the α_2 coefficient will be more pronounced than that of α_1, the effective gain $\alpha_1 - \alpha_2$ at low fields will be increasing instead of decreasing with the field, and the plot of $\alpha_1 - \alpha_2$ will be non-monotonic.

We now explain the hysteresis phenomena on the basis of Fig. 2. For this purpose we consider the case of hysteresis when a discharge current I in the amplifying medium (Fig. 1b) is swept through its range of values. Let the $\alpha_1 - \alpha_2$ plot pass successively through positions 2, 3, 4, 5, and 6 (Fig. 2) when the discharge current and consequently α_1 decrease. At the same time the field amplitude smoothly varies from E_2 to E_5, except for curve 6, for which (1.1) has no solution, and the only possible state of the system is that with E = 0. This means that the generation terminates abruptly at the time when the plot of $\alpha_1 - \alpha_2$ is no longer tangent to the straight line f. The current scan direction under consideration corresponds to curve 1 in Fig. 1b.

When the current is swept in the opposite direction there is no generation in the initial position (curve 6). Neither does generation occur in positions 5 and 4, although (1.1) then has a stable solution. For the generation to occur we must have some "priming" field that usually is of a fluctuational origin. Since for curves 5 and 4 losses exceed gain at low fields, $\alpha_1(0) - \alpha_2(0) < f$, the required priming field (E_5 and E_4' respectively in the cases under consideration) is not low and generation due to fluctuational "priming" is practically improbable. Generation arises abruptly only after position 3 is reached, when $\alpha_1(0) - \alpha_2(0) = f$ and any low "priming" field within some stabilization period converts the system to a stable state $E = E_3$. The output power in this and in all the subsequent points is the same as that observed in the opposite current scanning direction. The current scanning direction considered here corresponds to curve 2 in Fig. 1b.

Curves 2–6 in Fig. 2 differ comparatively little in shape. As a result the plot of $\epsilon(I)$ in Fig. 1b is a monotonically increasing current function. However the existence of a hysteresis region depends only on the behavior of the function $\alpha_1(E^2) - \alpha_2(E^2) - f$ near the point E = 0. Indeed, all the conditions for hysteresis will remain in force if only we demand that the derivative of $\alpha_1 - \alpha_2$ be positive in the zero point as the function $\alpha_1 - \alpha_2 - f$ passes through zero value. Hysteresis always exists when these conditions are met. On the other hand the plot of $\epsilon(I)$ can be monotonic or nonmonotonic depending on the degree of difference among the curves in Fig. 2. The following discussion shows that our assumptions concerning the shape of the curves in Fig. 2 are readily verifiable by experiment.

Consequently the assumptions underlying Fig. 2 explain both the fact that generation power depends on the current scanning direction in the discharge tube and the presence of abrupt jumps at the start and termination of generation (Fig. 1b).

A more detailed description of the phenomenon and the interpretation of the generation power peak and frequency hysteresis (Fig. 1a) require explicit expressions for the gain and absorption coefficients. Consideration of the nonlinear properties of the medium in the form of the first nonvanishing correction (such as it is done by Lamb[4]) is no longer sufficient for our purpose, since this yields rectilinear plots in Fig. 2. Therefore we use expressions that include fourth-order field amplitude terms for the coefficients α_1 and α_2. Then (1.1) has the form

$$y(\varepsilon) = a\varepsilon^2 - b\varepsilon + c = 0, \tag{1.2}$$

where $\epsilon = \sigma_1 E^2$, and the coefficients a, b, c depend on the frequency, relaxation characteristics of the atom, and excitation intensity of the system. Figure 2 shows that in the approximation of (1.2) the hysteresis region corresponds to completely determined signs of the coefficients: $a < 0$, $b < 0$, and $c < 0$, i.e., the signs of the coefficients are determined by the absorbing and not the active component of the oscillator. The end of generation (the extreme left-hand point of curve 1 in Fig. 1b) occurs when the discriminant in (1.2) vanishes:

$$b^2 = 4ac. \tag{1.3}$$

The "ignition" point of generation (the extreme right-hand point of curve 2 in Fig. 1b) occurs when coefficient c turns to zero. Thus in the region of the hysteresis

$$a < 0, \quad -\sqrt{4ac} \leqslant b < 0, \quad c \leqslant 0. \tag{1.4}$$

Of the two roots of (1.2) the system stability condition ($dy/d\epsilon < 0$) selects the root

$$\varepsilon = (b - \sqrt{b^2 - 4ac}) \,/\, 2a. \tag{1.5}$$

According to the experimental conditions[1,2] we assume that the Doppler line width $k\bar{v}$ is much larger than all the relaxation constants. According to[5] the spatial inhomogeneity of the medium due to saturation shows up to an insignificant degree and is not taken into account. Atomic diffusion in the velocity space due to velocity changes in collisions[6,7] is also neglected. We then obtain the following expressions for the coefficients a, b, and c:

$$c = N_1 - N_2 - 1 - \left(\frac{\Omega - \Delta}{k\bar{v}}\right)^2,$$

$$b = -\frac{1}{2}\left\{N_1\left[1 + L\left(\frac{\Omega - \Delta_1}{\gamma_1}\right)\right] - N_2\beta\left[1 + L\left(\frac{\Omega - \Delta_2}{\gamma_2}\right)\right]\right\},$$

$$a = \frac{3}{8}\left\{N_1\left[1 + L\left(\frac{\Omega - \Delta_1}{\gamma_1}\right) + 2L^2\left(\frac{\Omega - \Delta_1}{\gamma_1}\right)\right]\right.$$

$$\left. - N_2\beta^2\left[1 + L\left(\frac{\Omega - \Delta_2}{\gamma_2}\right) + 2L^2\left(\frac{\Omega_2 - \Delta_2}{\gamma_2}\right)\right]\right\},$$

$$\beta = \frac{\sigma_2}{\sigma_1} = \frac{\gamma_1}{\gamma_2}\frac{\gamma_{2m}^{-1} + \gamma_{2n}^{-1}}{\gamma_{1m}^{-1} + \gamma_{1n}^{-1}} \qquad N_i = \alpha_i(0)/f, \qquad \Delta = \frac{N_1\Delta_1 - N_2\Delta_2}{N_1 - N_2}$$

$$L(x) = \frac{1}{1 + x^2}. \tag{1.6}$$

Here the subscripts i = 1, 2 refer all quantities to the active or passive components respectively, N_i is the population difference expressed in the usual threshold units, and Δ_i is the line shift. The frequency Ω is measured from the transition frequency ω_{mn}. We note that expansion (1.2) is applicable when the dimensionless radiation intensity ϵ is small both in the active component

$$\varepsilon \ll 1, \tag{1.7}$$

and in the passive component

$$\beta\varepsilon \ll 1. \tag{1.8}$$

If the ratio β of the saturation parameters of the passive and active components is large then the second limitation can prove to be far more rigid and the first to be insignificant.

2. CURRENT HYSTERESIS

It is readily apparent from (1.6) that the hysteresis of emission power can be obtained by varying a number of parameters (N_i, Ω, f, $k\bar{v}$). From the experimental viewpoint however the most interesting are the populations N_i and frequency Ω. N_i can be readily varied by varying currents in the active or passive components of the laser while the remaining parameters are practically constant. Therefore the hysteresis accompanying the variation of N_i is called the current hysteresis. The frequency Ω can also be scanned by standard methods. In this case we use the term frequency hysteresis and discuss it in the next section.

The frequency dependence of the coefficients a, b, and c is not significant in current hysteresis; we thus consider generation only in the center of the line without taking the shifts into account: $\Omega = \Delta_1 = \Delta_2 = 0$. In this case the coefficients assume a simple form

$$\begin{gathered} c = N_1 - N_2 - 1, \quad b = N_1 - N_2\beta, \\ a = {}^3/_2(N_1 - N_2\beta^2). \end{gathered} \tag{2.1}$$

The generation power $\epsilon(N_1)$ is considered as a function of the concentration N_1 of the emitting atoms. Figure 3 shows a series of characteristic curves corresponding to various numbers of absorbing atoms N_2. Curve 1 represents the case of ordinary generation when $N_2 = 0$, the coefficients a and b are of the same order, and due to (1.7) the term $a\epsilon^2$ in (1.2) can be neglected. Here

$$\varepsilon \cong \frac{c}{b} = \frac{N_1 - 1}{N_1} \cong N_1 - 1. \tag{2.2}$$

Curve 3 corresponds to a value $N_2 = N_2^0$ that turns b and c simultaneously to zero at a certain point $N_1 = N_1^0$:

$$N_1^0 = \beta / (\beta - 1), \quad N_2^0 = 1 / (\beta - 1). \tag{2.3}$$

Such a point exists only when $\beta > 1$, corresponding to a high saturation in the passive component. Under this condition, that is now assumed satisfied, the coefficient $a(N_1^0)$ is negative and according to (1.5) we have near the point N_1^0

$$\varepsilon \cong \sqrt{-c/a} = \sqrt{\frac{2}{3(\beta-1)} \frac{N_1 - N_1^0}{N_1^0}}. \tag{2.4}$$

We note that N_1^0 is the threshold population in the presence of absorption N_2^0. Thus a characteristic feature of the point (2.3) is the square-root dependence of emission power on the population excess above threshold. We also note that (2.3) affords us the opportunity to determine experimentally the β parameter. To achieve this we measure the ratio of threshold values of N_1 for the curves 1 and 3.

Curve 2 in Fig. 3 corresponds to $0 < N_2 < N_2^0$. The coefficient $b > 0$ and hysteresis effects are absent in this region of N_2 values.

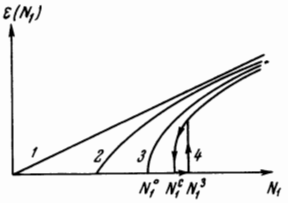

FIG. 3. Generation power ϵ as a function of the number of emitting atoms N_1 with the number of absorbing atoms N_2 remaining fixed. Curve $1 - N_2 = 0$; $2 - 0 < N_2 < N_2^0$; $3 - N_2 = N_2^0$; $4 - N_2 > N_2^0$.

Curve 3 is the boundary between the non-hysteresis curves of type 2 and those of type 4 for which $N_2 > N_2^0$. In the latter case $b < 0$ and consequently hysteresis is present. We find the width of the hysteresis region and the values of jumps in ϵ at the boundary of this region. The right- and left-hand boundaries of the region ("ignition" points N_1^i and termination points N_1^t) are determined by the generation conditions $c = 0$ and $b^2 = 4ac$ respectively (see (1.4)); hence

$$\frac{N_1^i - N_1^0}{N_1^0} = \frac{\eta_2}{\beta}, \qquad \frac{N_1^i - N_1^t}{N_1^0} = \frac{\beta - 1}{6\beta^2}\eta_2^2; \qquad \eta_2 = \frac{N_2}{N_2^0} - 1. \tag{2.5}$$

The values of power jumps ϵ_i and ϵ_t at these points are

$$\varepsilon_i = \frac{b}{a} \cong \frac{2}{3\beta}\eta_2, \qquad \varepsilon_t = \frac{b}{2a} = \frac{1}{2}\varepsilon_i. \tag{2.6}$$

The generation power near the termination point varies in the characteristic square-root manner as in the case of curve 3 (Fig. 3):

$$\varepsilon = \varepsilon_t\{1 + \sqrt{(N_1 - N_1^t) / (N_1^3 - N_1^t)}\}. \tag{2.7}$$

According to (2.5) and (2.7) the basic parameters of the hysteresis region are determined by η_2, i.e., by the excess of N_2 over the critical value of N_2^0. Jumps in emission power at the generation "ignition" and termination points and the distance between the "ignition" point N_1^i and point N_1^0 are proportional to η_2. On the other hand the width of the hysteresis region is proportional to η_2^2. We finally note that the left-hand jump is half as small as the right-hand one. This conclusion and the square-root dependence of ϵ near the termination point are confirmed by experiment (see Fig. 1b).

Let us emphasize that by virtue of (1.8) the formulas (2.5)–(2.7) are valid for $\eta_2 \ll 1$. This follows directly from a comparison of (2.6) and (1.8) for example.

In a similar manner we can consider ϵ as a function of the number of absorbing atoms N_2 when the values of N_1 are constant. This corresponds to a change of current in the passive component of the laser while the current in the active component is constant. The resulting plots are similar to the curves in Fig. 3 if N_2 instead of N_1 is laid off along the abscissa axis. The critical values of N_1^0 and N_2^0 remain of course the same. The width of the hysteresis region then turns out to be

$$\frac{N_2^t - N_2^i}{N_2^0} = \frac{\beta(\beta - 1)}{6}\eta_1^2, \qquad \eta_1 = \frac{N_1}{N_1^0} - 1, \tag{2.8}$$

and the jump values are

$$\varepsilon_i = 2\varepsilon_t = {}^2/_3\eta_1. \tag{2.9}$$

In this case the condition (1.8) that controls the applicability of approximation (1.2) postulates that $\eta_1 \ll \beta^{-1}$. In spite of this the relative width of the hysteresis region (2.8) can be larger (approximately β times) than the relative width given by (2.5). This is clearly due to the fact that the number of absorbing atoms N_2^0 is β times

smaller than the number of emitting atoms. Therefore it seems experimentally more convenient to vary the current in the passive cell.

3. FREQUENCY DEPENDENCE OF OUTPUT POWER

Frequency scanning produces fairly varied shapes of the power plots of $\epsilon(\Omega)$, since a large number of parameters (β, γ_i, Δ_i, N_i, etc.) participate in the expressions for the coefficients a, b, and c. Furthermore the frequency dependence of a, b, and c is more complex than the dependence on N_i. We are therefore limited to the consideration of some special cases. We assume that

$$\beta = \sigma_2/\sigma_1 \gg 1, \quad \tau = \gamma_1/\gamma_2 \gg 1, \tag{3.1}$$

which corresponds to a large collision broadening of the line in the active component of the laser. N_1 and N_2 can be conveniently replaced by other parameters:

$$n = N_2/N_1, \quad \zeta = 1 - n - 1/N_1. \tag{3.2}$$

It can be shown that the applicability condition (1.8) for the expansion (1.2) requires, in addition to the obvious $\zeta\beta \ll 1$, that the additional inequality be satisfied

$$n\beta - 1 \ll 1, \tag{3.3}$$

if $n\beta > 1$. Therefore by virtue of (3.1) and (3.2) we must always have

$$n \ll 1, \quad N_1 - 1 \ll 1. \tag{3.4}$$

Because of (3.4) the shifts Δ and Δ_1 practically coincide and can be regarded as zero without loss of generality.

If the frequency is measured in units of γ_1 and all coefficients are divided by N_1 (which obviously does not affect the end results) we obtain the following instead of (1.6):

$$c = \zeta - x^2/u, \quad x = \Omega/\gamma_1, \quad u = (k\bar{v}/\gamma_1)^2,$$
$$b = {}^1/_2\{1 + L(x) - n\beta[1 + L(\tau(x-\delta))]\}, \quad \delta = \Delta_2/\gamma_1,$$
$$a = {}^3/_8\{1 + L(x) + 2L^2(x) - n\beta^2[1 + L(\tau(x-\delta)) + 2L^2(\tau(x-\delta))]\}. \tag{3.5}$$

The product ζu determines the points where c = 0. Therefore the quantity ζ can be verified from the distance between the generation starting points (equal to $2\sqrt{\zeta u}$).

We first consider $\epsilon(x)$ for comparatively small absorptions where $1 - n\beta$ is not too small and $b^2 \gg 4ac$ at all frequencies. Then

$$\varepsilon \cong \frac{c}{b} = \frac{2}{u}\frac{\zeta u - x^2}{1 - n\beta + (1+x^2)^{-1}}\left[1 + \frac{h}{1 + \tau'^2(x-\delta)^2}\right], \tag{3.6}$$

$$h = \frac{n\beta/2}{1 - n\beta - \delta^2/2(1+\delta^2)}, \quad \tau'^2 = \tau^2\frac{1 - n\beta/2 - \delta^2/2(1+\delta^2)}{1 - n\beta - \delta^2/2(1+\delta^2)}. \tag{3.7}$$

According to (3.6), the function $\epsilon(x)$ contains two scale parameters: $\sqrt{\zeta u}$ and $1/\tau'$. If $\sqrt{\zeta u} \gg 1$ (i.e., the width γ_1 is much smaller than the generation region) the plot of $\epsilon(x)$ has a typical "Lamb dip" that is defined by the denominator in (3.6) and that can be given the form

$$\left[1 - n\beta + \frac{1}{1+x^2}\right]^{-1} = \frac{1}{1-n\beta}\left[1 - \frac{1/(2-n\beta)}{1 + x^2(1-n\beta)/(2-n\beta)}\right] \tag{3.8}$$

Consequently the introduction of absorption increases in general both the depth and the width of the "dip." This is obviously due to the nonresonance portion of saturation in the passive cell (the term $-n\beta$ in the expression (3.5) for b). Lisitsyn and Chebotaev[11] did not observe the "dip" (curve 1 in Fig. 1a), i.e., the parameter ζu was of the order of unity; this is implied in the following.

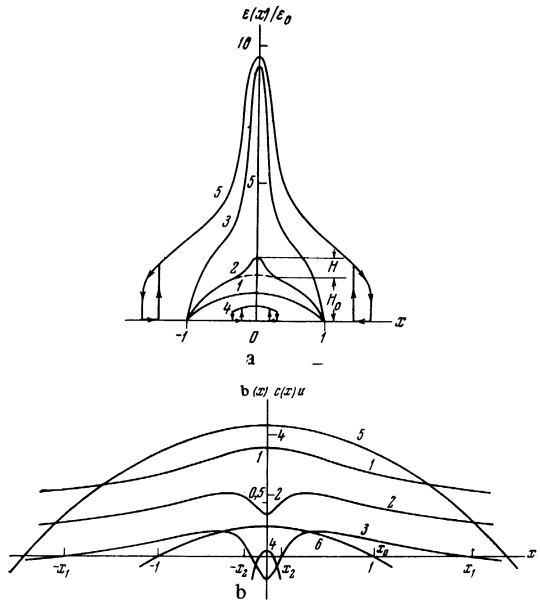

FIG. 4. a – generation power ϵ as a function of frequency $x = \Omega/\gamma_1$ in the symmetric ($\delta = 0$) case; $\tau = \gamma_1/\gamma_2 = 6$, $\beta = 10$, $\zeta = 2 \times 10^{-3}$. Curve 1 – $n\beta = 0$; 2 – $n\beta = 0.6$; 3 – $n\beta = 1.2$. Curves 4 and 5 are not to scale; $h = H/H_0$. b – Frequency dependence of the coefficients b(x) (curves 1 – 3) and c(x) curves 4 – 6); $\tau = 6$. Curve 1 – $n\beta = 0$; 2 – $n\beta = 0.6$; 3 – $n\beta = 1.2$. Curve 4 is not to scale.

The factor in brackets in (3.6) indicates the existence of a power peak with a dispersive shape, a width of $1/\tau' < 1/\tau \ll 1$ and relative height h (Fig. 4a). This peak is due to that resonance portion of saturation in the passive cell (the term $-n\beta L[\tau(x-\delta)]$ in the expression (3.5) for b) which causes a minimum in the plot of b(x) (if $n\beta\tau^2 > 1$, Fig. 4b, curve 2). An increase in absorption causes an increase of the height of the peak as well as a narrowing of the peak and an increase of power ϵ_m in the maximum[2)]. In the symmetric case when $\delta = 0$ we have

$$\frac{\varepsilon_m - \varepsilon_0}{\varepsilon_0} = \frac{n\beta}{1-n\beta} = 2h, \frac{1}{\tau'} = \frac{1}{\tau}\sqrt{\frac{1-n\beta}{1-n\beta/2}} = \frac{1}{\tau}\sqrt{\frac{2}{1+\varepsilon_m/\varepsilon_0}}, \tag{3.9}$$

where ϵ_0 is power in maximum for $n\beta = 0$. If $\delta \neq 0$ the plot of $\epsilon(x)$ becomes asymmetric and the peak maximum occurs near $x = \delta$.

It follows from (3.7) that (3.6) is no longer valid if

$$b(x = \delta) = 1 - n\beta - \delta^2/2(1+\delta^2) \to 0.$$

This is due to the fact that the term 4ac dropped out in the transition from (1.5) to (3.6). The exact expression at $x = 0$ and for $\delta = 0$ has the form

$$\frac{\varepsilon_m - \varepsilon_0}{\varepsilon_0} = \frac{2}{1 - n\beta + [(1-n\beta)^2 - 6(1-n\beta^2)\zeta]^{1/2}} - 1. \tag{3.10}$$

Since $\zeta\beta \ll 1$ the term $6(n\beta^2 - 1)\zeta$ is significant only for small

$$|n\beta - 1| \sim \sqrt{6|n\beta^2 - 1|}\zeta \ll 1.$$

[2)] Absorption increase with constant ζ implies a corresponding gain increase (see (3.2)) that is also the cause of power increase.

Therefore we set $n\beta = 1$ in this term and proceed from (3.10) to the expression

$$\frac{\varepsilon_m - \varepsilon_0}{\varepsilon_0} = \frac{2}{1 - n\beta + [(1-n\beta)^2 + \chi]^{1/2}} - 1, \quad \chi = 6(\beta - 1)\zeta. \tag{3.11}$$

We can readily show that (3.11) leads to a monotonic increase of ϵ_m with $n\beta$ and we have $\epsilon_m/\epsilon_0 = 2/\sqrt{\chi}$ at the characteristic point $n\beta = 1$. When $1 \gg n\beta - 1 \gg \sqrt{\chi}$ (3.11) yields

$$\varepsilon_m / \varepsilon_0 \cong 4(n\beta - 1) / \chi,$$

i.e. the rise of ϵ_m (with $n\beta$) is again linear but this time with a much larger slope than when $n\beta \ll 1$ ($4/\chi$ times). Our initial expansion of (1.2) is no longer valid with any further increase of $n\beta$. However, we can show that ϵ_m always grows with increasing $n\beta$.

We now analyze frequency hysteresis and first consider the symmetric case of $\delta = 0$. The general conditions (1.4) of the hysteresis effects require that all the coefficients a, b, and c be negative. If $n\beta > 1$ the coefficient b(x) becomes negative (Fig. 4b, curve 3) within the regions

$$|x| < x_2 \cong \tau^{-1}\sqrt{2(n\beta - 1)} \quad \text{(first region)}$$

and

$$|x| > x_1 \cong (n\beta - 1)^{-1/2} \gg 1 \quad \text{(second region)}.$$

The coefficient a is a priori negative in these regions while the coefficient $c < 0$ when $|x| > x_0 = \sqrt{\zeta u}$. In the intermediate region $x_2 < |x| < x_1$ hysteresis is impossible because $b > 0$. The possibility of hysteresis occurring in the first and second regions depends on the quantity $x_0 = \sqrt{\zeta u}$. If $x_0 < x_2$ hysteresis will exist in the region $x_0 < |x| < x_2$ (curves 4 in Fig. 4a and b). If $x_0 > x_1$ hysteresis is also possible in $|x| > x_0$ (curves 5 in Fig. 4a and b). On the other hand, if $x_2 < x_0 < x_1$ (curve 6, Fig. 4b), hysteresis is impossible even if all coefficients are negative in the second region.

Indeed in this case the coefficient c turns to zero at a point where b is still positive. Therefore when the frequency is scanned (in the direction of increasing $|x|$) we have the usual termination of generation (without a jump and without the square root singularity) at the point $|x| = x_0$ and generation can no longer occur with increasing $|x|$. When the scanning direction is reversed (decreasing $|x|$) generation occurs at the same point at which it terminated. Thus the curves in Fig. 4b exhaust all cases of hysteresis for $\delta = 0$ that are possible within the second power (in terms of ϵ) expansion of (1.2).

Figure 4b indicates the hysteresis regions in a more general case regardless of the validity of (1.2). We note that the general conditions of hysteresis postulate merely a definite behavior of the $\alpha_1 - \alpha_2 - f$ function near the point $\epsilon = 0$ (see discussion of Fig. 2), i.e., that the coefficient c should turn to zero at a point where $b < 0$. Consequently we can use Fig. 4b regardless of the magnitude of $n\beta$ to define the frequency regions that permit hysteresis.

It is readily shown that when the condition

$$n\beta > \{\sqrt{2} - [1/(\tau + \sqrt{2})]\}^2 \tag{3.12}$$

is met coefficient b is negative for all frequencies and hysteresis is observed for any value of ζ.

Let the maxima of the amplification and absorption lines be shifted with respect to one another and $\delta \neq 0$. The characteristic function b(x) is given in Fig. 5b. As before hysteresis is observed if the points $\pm x_0 = \pm\sqrt{\zeta u}$ for which $c = 0$ fall within the regions

$$x < x_1, \quad x_2 < x < x_3, \quad x_4 < x, \tag{3.13}$$

where $b < 0$. However in contrast to the case of $\delta = 0$ the plots of $\epsilon(x)$ are asymmetric and hysteresis can either be absent or be present on one side or on both sides.

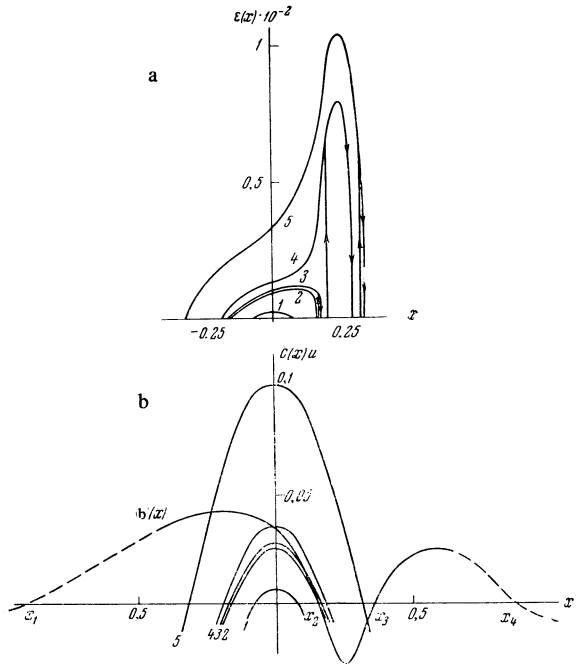

FIG. 5. a – Frequency dependence of generation power ϵ for various values of gain excess over threshold and a shift between the centers of absorption and amplification lines. b – Frequency dependence of the coefficients b(x) and c(x) (curves 1 – 5). The dashed portion of the curve b(x) is not to scale. $\delta = \frac{1}{4}$; $\tau = 8$; $n\beta = 1.2$. Curve 1 – $x_0 = 0.08$; 2 – $x_0 = 0.158$; 3 – $x_0 = 0.164$; 4 – $x_0 = 0.20$; 5 – $x_0 = 0.32$.

We trace the sequence of the $\epsilon(x)$ plots of the above types as x_0 varies. For the sake of definiteness let $b > 0$ at the point $x = 0$ (Fig. 5b). Then hysteresis is altogether absent when $x_0 < x_2$ (curve 1), is present only on the right-hand side of the plot when $x_2 < x_0 < x_3$ (curves 3 and 4), and is again absent in the case when $|x_1|, x_4 > x_0 > x_3$. As x_0 increases further the phenomenon depends on the relation between $|x_1|$ and x_4. We can show that $|x_1| > x_4$. Consequently as x_0 increases hysteresis first occurs on the right-hand side of the plot of $\epsilon(x)$ (when $|x_1| > x_0 > x_4$) and only later on the left-hand side. Thus hysteresis effects always begin on the side of the plot of $\epsilon(x)$ towards which the power peak is shifted ($x \cong \delta$) and appear on the opposite side only in the course of a further increase of x (or of $n\beta$). The experiments[1] failed to reveal a single exception from this rule.

Let us examine in greater detail the variation of the plot of $\epsilon(x)$ with increasing ζ or, more conveniently, $x_0 = \sqrt{\zeta u}$. If $x_2 - x_0 > 0$ is sufficiently large (curve 1 in Fig. 5b), $\epsilon \cong c/b$, the coefficient b changes relatively little, and the plot of $\epsilon(x)$ is almost symmetric (curve 1 in Fig. 5a). As the distance $x_2 - x_0$ decreases between the zeros of coefficients b and c, the variation of b as-

sumes an increasing significance within the interval $-x_0$, x_0 and the plot of $\epsilon(x)$ becomes asymmetric. To investigate the plots near x_2 for small $|x_2 - x_0|$ we expand b and c in powers of $x - x_2$:

$$\varepsilon / \varepsilon_1 = y + [(y-\eta)^2 - 2\eta(y_0 + \eta/2)]^{1/2},$$

$$y = x - x_2, \quad y_0 = x_0 - x_2, \quad \eta = 4\frac{|a(x_2)|}{b'^2(x_2)}\sqrt{\frac{\zeta}{u}}, \quad \varepsilon_1 = \frac{|b'(x_2)|}{2|a(x_2)|} \quad (3.14)$$

The function (3.14) is illustrated in Fig. 6 for four characteristic values of y_0. Curve 1 corresponds to $y_0 = 0$, the case when the zeros of coefficients b and c coincide. Here the generation terminates at the point $y = y_0$, power ϵ turns to zero according to the square-root law typical of the pre-hysteresis regime

$$\varepsilon \infty \sqrt{-2\eta y} = \sqrt{-2\eta(x - x_0)},$$

and the plot of $\epsilon(x)$ assumes a sharply asymmetric shape as a whole (curves 2 in Fig. 5b and a).

If $y_0 > 0$ then c turns to zero in the region where $b < 0$ and hysteresis takes place according to the general conditions. However the shape of the plots of $\epsilon(x)$ significantly depends on the relationship between y_0 and the parameter η. When $0 < -y_0 < \eta/2$ the discriminant in (3.14) turns to zero at the point

$$y_c = \eta - \sqrt{\eta(\eta + 2y_0)},$$

and generation terminates abruptly (curve 2 in Fig. 6). The start of generation (frequency scanned from right to left) is as usual at the point y_0. The entire plot of $\epsilon(x)$ (see curves 3 in Fig. 5a and b) is sharply asymmetric as before and the width of the hysteresis region is very small:

$$\eta + y_0 - \sqrt{\eta(\eta + 2y_0)} < \eta/2 \ll 1.$$

Now let $-y_0 \geq \eta/2$. Under these conditions the discriminant in (3.14) cannot be negative and generation power sharply rises to the right of the point $y = \eta$ (curves 3 and 4 in Fig. 6). Figure 5b shows (curve 4) that this is accompanied by a power peak with a maximum near $x = \delta$. An abrupt termination of generation (the discriminant vanishes near the point x_3) occurs on the right-hand side of the peak. The power ϵ_m at the peak maximum depends on the relationship between the parameter χ and the minimum value of b just as in the case of $\delta = 0$. In particular if $b^2(\delta) \gg 4a(\delta)c(\delta)$, i.e.,

$$n\beta - 1 - \delta^2/2(1+\delta^2) \gg \sqrt{\chi}(\delta^2/x_0^2 - 1)^{1/2},$$

then $\epsilon \cong b/a$ and ϵ_m is practically independent of ζ (compare curves 4 and 5 in Fig. 5a). We emphasize that with a small excess of y_0 over $\eta/2$ the entire peak is within the hysteresis region whose width is comparable to $x_3 - x_2 \gg \eta$. Thus in the case of $\delta \neq 0$ the width of the hysteresis region changes abruptly at the point $-y_0 = \eta/2$.

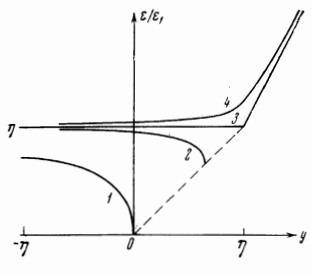

FIG. 6. The shape of function ϵ (3.14) for various values of y_0; curve 1 – $y_0 = 0$; 2 – $y_0 = 4/9\eta$; 3 – $y_0 = \eta/2$; 4 – $y_0 = 0.52\eta$.

A significant increase of y_0 (in comparison to η) shifts the hysteresis region in the direction of x_3; the region narrows down and completely vanishes when $x_0 = x_3$. Finally when $x_0 > x_4$ and $x_0 > -x_1 > x_4$ hysteresis regions appear consecutively in the right- and left-hand sides of the plot of $\epsilon(x)$. In the course of these changes the power peak near $x = \delta$ continues although its relative height decreases with increasing x_0.

4. CONCLUSIONS

We first consider the problem of the relation between the above theory and experiment. The work was based on the following three assumptions: (1) nonmonotonic dependence of the effective gain $\alpha_1 - \alpha_2$ on the squared field amplitude ϵ; (2) the use of expansion of $\alpha_1 - \alpha_2$ in powers of ϵ including ϵ^2; (3) a definite collision model for the computation of the expansion coefficients a, b, and c. These three assumptions do not carry equal weight. The first implies the very fact of the hysteresis effect, the abrupt change of generation power at the boundaries of the hysteresis region, and the square-root dependence of power near the generation termination point and before the onset of hysteresis. All these phenomena are observable and constitute a qualitative verification of the theory. The retention of the ϵ^2 terms in the $\alpha_1 - \alpha_2$ expansion is the first approximation in the description of the hysteresis effects. This approximation was selected exclusively for the sake of analytic simplicity and in order to encompass the broad range of phenomena for which such an approximation is still adequate. Nevertheless it is a serious limitation and in some cases Lisitsyn and Chebotaev[1,2] reached powers high enough to make our approximation appear unacceptable. The expansion we used is not suitable also in the solution of the important problem of the power limits attainable in lasers with an absorbing cell. The analysis of this problem requires exact expressions for $\alpha_i(\epsilon)$.

The most detailed part of the theory is the expression (1.6) for the coefficients a, b, and c. The width and height of the power peak, the sequence of appearance of frequency hysteresis accompanying the variation of excitation, and the widths of the current and frequency hysteresis regions are all defined by the explicit form of the coefficients a, b, and c. The majority of these results have had no quantitative confirmation at this time. Insofar however as the first two assumptions cannot raise any doubts such a proof would merely constitute a validation of our concepts concerning relaxation phenomena in the active and absorbing media.

In Sec. 3 we were limited to the special case where the line widths and saturation parameters are markedly different in the two laser components, $\tau \gg 1$, $\beta \gg 1$. We now consider some other possible situations. So far we assumed that amplification and absorption occur at the same transition but with different gas pressures. The condition $\tau \gg 1$ here implies $\beta \gg 1$ and vice versa (see (1.6)). The absorbing gas can obviously differ from the amplifying gas. In that case β contains the squared ratio of the matrix elements of the dipole moment and the parameters τ and β are not very rigidly bound[3], i.e.,

[3] We note that the value of β can also be varied with constant τ by focusing or defocusing the field in one of the laser components. This possibility was not taken into account in (1.6).

the condition $\beta > 1$ or $\beta < 1$ can be satisfied for any value of τ.

It is clear from Secs. 2 and 3 that the hysteresis conditions limit only the value of β. For example if $\delta = 0$ it is necessary that $\beta > 1$ and the ratio of line widths τ is arbitrary. Variation of τ obviously does not introduce qualitative changes into the plots of $\epsilon(I)$ (Fig. 3). On the other hand the frequency dependence of power will be quite different since the plots of the coefficients b(x) and a(x) are strongly dependent on τ. In particular, when $\beta \gg 1$ and $\tau \ll 1$, we can choose the conditions so as to have two power peaks in $\epsilon(x)$ at the boundaries of the generation region.

In conclusion we note the nature of transient processes typical of lasers with an absorbing cell. The equation of motion

$$d\varepsilon / dt = (\alpha_1 - \alpha_2 - f)\varepsilon,$$

shows that the characteristic periods of variation of ϵ significantly depend on the shape of the function $\alpha_1 - \alpha_2 - f$. Therefore the introduction of an absorbing cell can strongly affect the time characteristics of the laser.

The above analysis shows that a gas laser with an absorbing cell is subject to numerous and unique phenomena that are of interest both in terms of their physics and applications. In addition to their use in spectroscopy and frequency stabilization systems[2,3] there are other possible applications of these phenomena. For example a laser with an absorbing cell operating in the hysteresis mode can serve as a memory element.

[1] V. N. Lisitsyn and V. P. Chebotaev, ZhETF Pis. Red. 7, 3 (1968) [JETP Lett. 7, 1 (1968)].

[2] V. N. Lisitsyn and V. P. Chebotaev, Zh. Eksp. Teor. Fiz. 54, 419 (1968) [Sov. Phys.-JETP 27, 227 (1968)].

[3] P. H. Lee and M. L. Skolnick, Appl. Phys. Lett. 10, 303 (1967).

[4] W. E. Lamb, Jr., Phys. Rev. 134, A1429 (1964).

[5] S. G. Rautian, Dissertation, FIAN, 1966.

[6] A. P. Kazantsev and G. I. Surdutovich, Trudy II simpoziuma po nelineĭnoĭ optike (Proceedings of the II Symposium on Nonlinear Optics), Novosibirsk, 1966.

[7] S. G. Rautian, Zh. Eksp. Teor. Fiz. 51, 1176 (1966) [Sov. Phys.-JETP 24, 788 (1967)].

Translated by S. Kassel
165